SAKARYA ÜNİVERSİTESİ

FEN BİLİMLERİ ENSTİTÜSÜ
DERGİSİ

Sakarya University Journal of Science
SAUJS

e-ISSN 2147-835X Period Bimonthly Founded 1997 Publisher Sakarya University
http://www.saujs.sakarya.edu.tr/

Title: Theoretical Investigation of the W(CO)6 and CO Selenization Process

Authors: Nadire NAYİR

Recieved: 2021-12-18 00:00:00

Accepted: 2022-02-19 00:00:00

Article Type: Research Article

Volume: 26
Issue: 2
Month: April
Year: 2022
Pages: 283-291

How to cite
Nadire NAYİR; (2022), Theoretical Investigation of the W(CO)6 and CO Selenization Process. Sakarya University Journal of Science, 26(2), 283-291, DOI: 10.16984/saufenbilder.1038357
Access link
https://dergipark.org.tr/tr/journal/1115/issue/69580/1038357

Sakarya University Journal of Science 26(2), 283-291, 2022

Theoretical Investigation of the $W(CO)_6$ and CO Selenization Process

Nadire NAYİR*[1]

Abstract

Detailed atomic-level insight into the mechanism of $W(CO)_6$ and CO selenization is essential for the fabrication of cheap and environmentally benign transition metal chalcogenides such as MoS_2 and WSe_2. Earlier discussions in literature have focused mainly on the CO methanation by sulfur and its derivatives but H_2Se mediated CO methanation at the atomic level is yet to be explored. First-principles calculations and ReaxFF-based molecular dynamics simulations are conducted here to explore the relative stabilities of intermediates formed during the gas-phase interactions of $W(CO)_6$ and H2Se, determined associated reaction energies and kinetic barriers. The methanation of CO, which is released from the organometal, by H_2Se is further investigated. The results indicate that the chain reactions of $W(CO)_6$ and H_2Se lead to the formation of a thermodynamically stable end product of $W(SeH)_2Se_2$. Depending on the temperature, $W(HSe)_2Se_2$ is expected to go through a last uphill reaction by releasing H2Se into the environment and evolving into a WSe_3 molecule. Additionally, the dehydrogenation of organometallic molecules is thermodynamically feasible but kinetically controlled, requiring a significant activation energy. When all CO groups are released from the W atom, the H_2 release from W-compund becomes nearly barrierless. Since CO radical groups are dominant byproducts formed during the MOCVD chain reactions but in a chalcogen rich environment, this work also shed light into the CO selenization during the growth of transition metal diselenides (e.g., WSe_2, $MoSe_2$, $CrSe_2$) and discusses the formation of potential products such as CSe_2, CH_4, H_2Se, CO, H_2O, Se_2.

Keywords: Density functional theory, ReaxFF molecular dynamics, $W(CO)_6$ and H_2Se interactions, CO methanation.

1. INTRODUCTION

Transition metal dichalcogenides (TMD) which belong to the emerging family of two-dimensional layered materials are a promising platform for a new generation of electronic and optoelectronic devices because of their unique physicochemical, optical, and electronic properties [1-6]. TMD is composed of layers that are coupled by weak van der Waals forces but have strong covalent bonds between the in-plane atoms. There are many techniques to fabricate such materials, e.g., atomic layer deposition [7-9], chemical vapor deposition/metal-organic chemical vapor deposition (MOCVD) [2, 10, 12], and molecular beam epitaxy [13-16]. Among them, MOCVD is a common method that is utilized for the synthesis of TMD materials.

---

* Corresponding author: nnayir@kmu.edu.tr

[1] Karamanoğlu Mehmetbey University, Kamil Özdağ Faculty of Science, Pyhsics Department

ORCID: https://orcid.org/0000-0002-3621-2481

Because it allows for control of the precursor ratio and flux and provides flexibility in precursor selection, it consequently enables the fabrication of high-quality, nearly single-crystalline TMD materials. MOCVD uses volatile metal-organic and chalcogen precursors that are injected into the chamber through separate inlets. This leads to complex physicochemical processes that initiate the deposition of TMD materials onto substrate. Even though this technique reduces the need for source heating because of the relatively high vapor pressures of hydrides, the elevated temperature is still required during growth to overcome energy barrier necessary to eliminate residual carbon from the metal precursors and promote chemisorption of metal and chalcogen by surface [2, 10, 11].

Despite tremendous progress on the MOCVD growth technique, the synthesis of large-scale, defect-free TMD materials with controllable thickness is still challenging for reasons such as the fact that the synthesis and characterization are costly and relatively slow, precursors are expensive and toxic, and the selection of substrate is restricted. This has therefore triggered theoretical modeling to shed new light on the design and fabrication of TMD-based devices at the atomistic level. To date, Xuan et. al [17] developed a multiscale framework as a combination of ReaxFF empirical potential and continuum fluid dynamics methods for the gas-phase kinetics of the MOCVD growth of WSe_2 from the gas precursors $W(CO)_6$ and H_2Se. However, to the best of the author's knowledge, there is no report yet on a detailed mechanism of the $W(CO)_6$ selenization at the DFT level and the CO selenization process has yet to be explored. In this study, the selenization of $W(CO)_6$ and CO is investigated using DFT and ReaxFF methods. A series of DFT calculations are conducted to extract a thermodynamically allowable pathway from $W(CO)_6$ and H_2Se gas-phase precursors to WSe_3. ReaxFF atomistic simulations are also performed to explore the impact of temperature on the adduct formation besides end-product derived from the $W(CO)_6$ and H_2Se chain chemical interactions. Following the results obtained at DFT and ReaxFF level, the CO methanation by H_2Se is further studied to provide insight into the relative stabilities of adducts formed during the MOCVD growth of WSe_2.

2. METHOD OF CALCULATIONS

Jaguar calculations: Nonperiodic QM calculations are performed via Jaguar[18] using the B3LYP functional and the LACV3P**++ effective core potential. **ReaxFF MD simulations:** Molecular dynamics (MD) simulations are performed using ReaxFF/ADF [19] based on the ReaxFF force field developed by Xuan et al [17]. A comprehensive review of the ReaxFF formalism can be found in Chenoweth et al.[20] The models in the figures are visualized using VESTA [21].

3. RESULTS AND DISCUSSION

3.1. Impact of H_2 formation on MOCVD growth of TMD growth

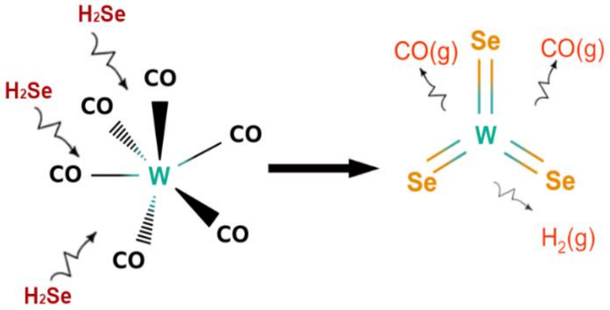

Figure 1 The initial and final product of MoCVD gas-phase reactions.

MOCVD gas-phase kinetic of TMD materials from volatile organometal and chalcogen precursors is a complicated process and heavily relies on numerous chemical reactions. In this study, the DFT calculations are conducted to track the chemical and structural evolution of the vaporized $W(CO)_6$ and H_2Se precursors to the end product of WSe_3 and to lay out the full picture of the thermodynamically favorable MOCVD reaction pathway (Figures 1-3). The chemical reactions are classified into three main groups: (i) CO dissociation from (ii) H_2Se binding to and (iii) H_2 elimination from $W(CO)_x(H_2Se)_y(HSe)_zSe_m$ molecule where x, y, z, m=0, 1, 2, 3, 4 (Figure 1), as also reported by Xuan et al. [17]

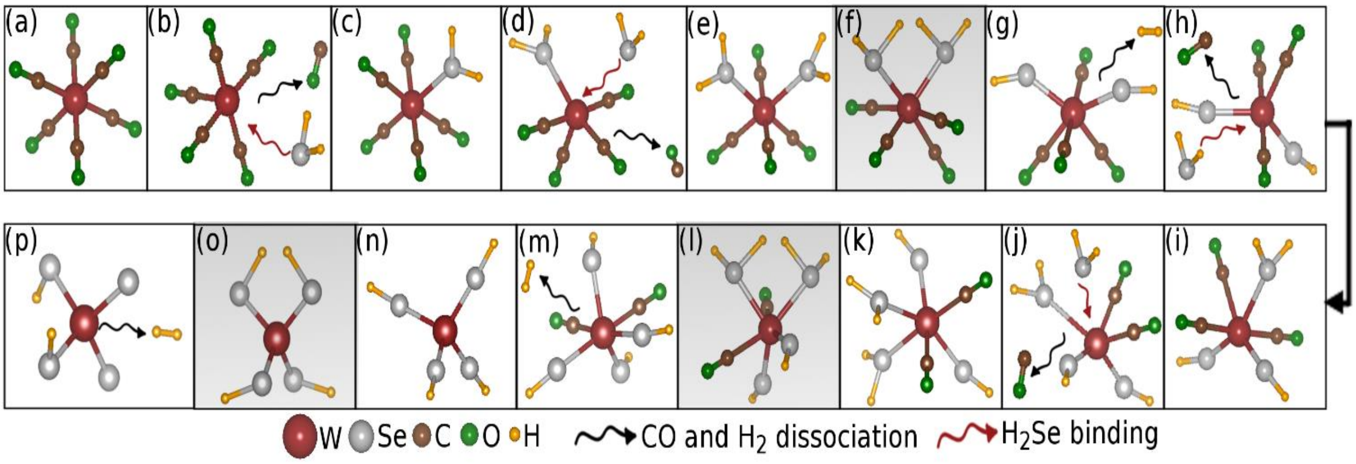

Figure 2 Ball-and-stick representations of the proposed MOCVD reaction pathway starting from (a) the dissociation of CO from $W(CO)_6$ and leading to (p) the thermodynamically stable end product, $W(SeH)_2Se_2$. (f, l, o) The three key transition states for H_2 formation are highlighted with a gray background.

As shown in Figure 2a-c, the MOCVD gas-reaction chain initiates with the loss of the first CO group from the $W(CO)_6$ molecule with dissociation energy of 1.79 eV, and then, continues with H_2Se binding to the W-metal. Losing the second CO group creates a new empty site for binding of the second H_2Se to the metal (Figure 2d,e), which leads to the bimolecular elimination of H_2 from $W(CO)_4(H_2Se)_2$ (Figure 2f,g). Then, the $W(CO)_4(HSe)_2$ molecule goes through two consecutive carbonyl dissociations, binds two more H_2Se (Figure 2h-j) molecules, and results in $W(CO)_2(HSe)_2(H_2Se)_2$ (Figure 2k). The presence of two hydrides weakly bonded to metal triggers the evolution of the $W(CO)_2(HSe)_2(H_2Se)_2$ molecule to $W(CO)_2(HSe)_4$. To reach this stable conformational state of $W(CO)_2(HSe)_4$, the $W(CO)_2(HSe)_2(H_2Se)_2$ molecule passes through a second transition state by releasing an H_2 molecule (Figure 2l,m). Subsequently, the resulting $W(CO)_2(HSe)_4$ molecule, loses the last two CO groups and degrades into $W(HSe)_4$ (Figure 2n). This molecule releases further an H_2 molecule (Figure 2o), finally evolving to the thermodynamically stable end product of $W(HSe)_2Se_2$ (Figure 2p). Figure 3a illustrates the proposed MOCVD reaction pathway starting from the gas-phase precursors $W(CO)_6$ and H_2Se and leading to the thermodynamically stable end product of $W(SeH)_2Se_2$ at the DFT level. Then, depending on the temperature, $W(HSe)_2Se_2$ goes through a last uphill reaction by releasing H_2Se into the chamber and evolves into the WSe_3 molecule with a net additional energy of 0.52 eV by following the reaction pathway shown in Figure 3b.

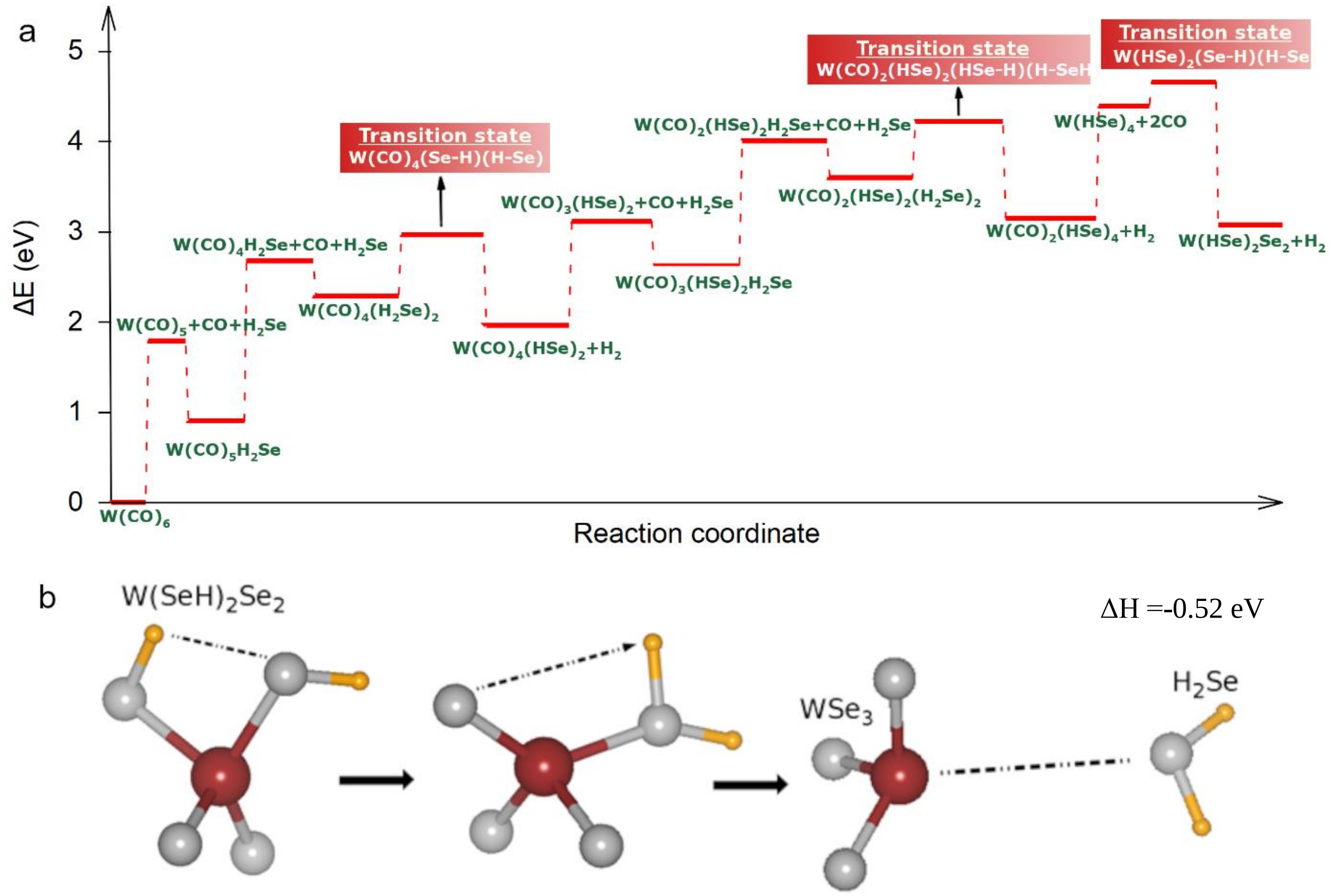

Figure 3 (a) DFT-based reaction pathways for MOCVD growth of WSe_2, starting from the gas precursors $W(CO)_6$ and H_2Se and leading to the thermodynamically stable end-product of $W(H_2Se)Se_2$. (b) Chemical evolution of WSe_3 and H_2Se from $W(SeH)_2Se_2$ with an entalphy energy of 0.52 eV, where dark red, gray and gold atoms are W, Se and H, respectively.

Additionally, as seen from Figure 3a, the H_2 elimination is an exothermic chemical event - in case that at least two H_2Se or HSe bind to a W metal, three key transition states are expected for H_2 release in the thermodynamically proposed MOCVD reaction pathway illustrated in Figures 2 and 3:

$$W(CO)_4\,(H_2Se)_2 \rightarrow W(CO)_4(HSe)_2 + H_2$$

$$\Delta H = -0.33\text{ eV},\;\; E_a = 0.68\text{ eV} \qquad (1)$$

$$W(CO)_2(H_2X)_2(HX)_2 \rightarrow W(CO)_2(HSe)_4 + H_2$$

$$\Delta H = -0.45\text{ eV},\;\; E_a = 0.62\text{ eV} \qquad (2)$$

$$W(HSe)_4 \rightarrow W(HSe)_2Se_2 + H_2$$

$$\Delta H = -1.32\text{ eV},\;\; E_a = 0.27\text{ eV} \qquad (3)$$

where ΔH and E_a are enthalpy and activation energies of the reactions above. These transition reactions result in thermodynamically more stable products of $W(CO)_4(HSe)_2$, $W(CO)_2(HSe)_4$ and $W(HSe)_2Se_2$ than the reactants of $W(CO)_4(H_2Se)_2$, $W(CO)_2(H_2Se)_2(HSe)_2$ and $W(HSe)_4$, suggesting that 2D-WSe_2 growth is thermodynamically favored. However, the results also show that dehydrogenation of organic molecule is kinetically hindered, requiring activation energy of 0.6 − 0.7 eV (Eqs. 1-2) to overcome the kinetic barrier for the H_2 elimination, indicating that the MOCVD growth of WSe_2 requires external energy (e.g., temperature and/or pressure) to accelerate the chemical reactions. Additionally, the reaction of

$$W(CO)_2(HSe)_2(H_2Se)_2 \rightarrow W(CO)_2(HSe)_2(Se{-}H)(H{-}Se)^{TS}$$

is considered as a rate-limiting reaction governing the MOCVD growth kinetics since the W-organic molecule encounters the highest energy barrier of 0.68 eV during the H_2 release. The willingness of the Se atom to lose the H atom decreases with the decrease of the number of CO ligands bound to a W atom. In case of losing all CO groups from the W atom, the H_2 release from the W-compund becomes nearly barrierless (0.27 eV in Eq. 3).

The combustion of $W(CO)_6$ with H_2Se molecules increase the CO concentration in the environment. Therefore, the CO methanation by H_2Se and potential intermediates are also expected to form during the MOCVD growth of WSe_2 and other transition metal diselenides such as $MoSe_2$, $CrSe_2$. Table 1 summarizes the proposed reactions for adduct formation and corresponding energies. Additionally, the proposed thermodynamically favored reaction pathway for CO methanation by H_2Se is as follows:

$$SeCO \rightarrow H_3CSeH \rightarrow CH_4 \rightarrow CSe_2 \qquad (4)$$

CSe_2 formation from the CO selenization is expected to realize in four stages:

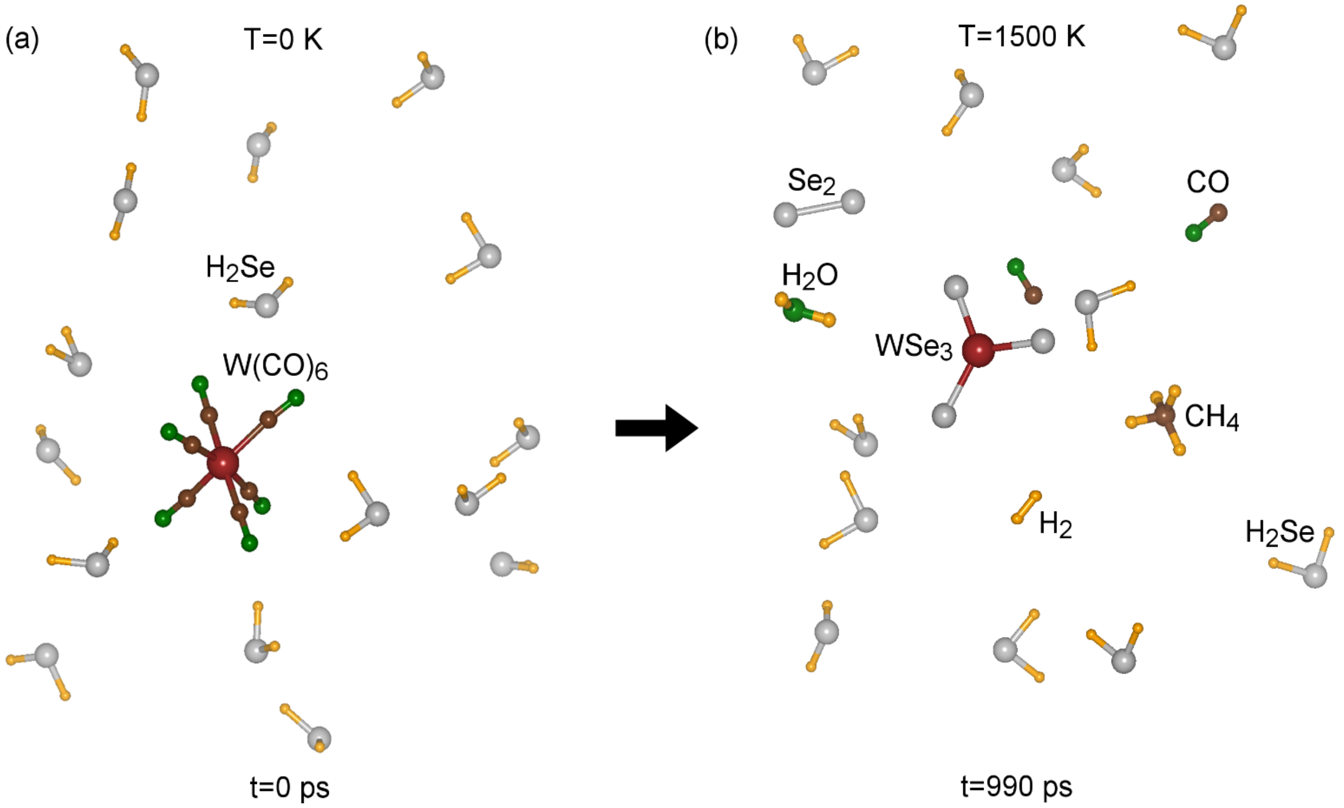

Figure 4 MOCVD gas-phase kinetic at 1500 K obtained from CVHD implemented ReaxFF-MD simulations. (a) The initial configuration of the simulation box which includes the gas-phase precursors $W(CO)_6$ and H_2Se and (b) the end- and by-products formed at 1500 K.

I) The pathway in Eq. 4 is expected to initiate with the attack by Se radical present on CO to form SeCO, which is thermodynamically favored.

$$CO + Se \rightarrow SeCO \qquad \Delta H = -3.62 \text{ eV}$$

Note that the HSe formation is catalyzed by organometal with vacancies, then two HSe molecules come together and form H_2Se and Se radical as seen below:

$$-W{=}Se + H_2Se \rightarrow -W{-}SeH + HSe$$

$$HSe + HSe \rightarrow H_2Se + Se$$

The SeCO formation by Se_2 and HSe manifest endothermic behavior. Additionally, even though the selenization reaction of CO by H2Se exhibits a slightly exothermic character (-0.07 eV), this is also kinetically hindered which requires activation energy of 1.96 eV to release an H_2 molecule.

$CO + Se_2 \rightarrow SeCO + Se \qquad \Delta H = 1.14$ eV

$CO + HSe \rightarrow SeCO + H \qquad \Delta H = 1.18$ eV

$CO + H_2Se \rightarrow OC{-}H_2Se\ (TS) \rightarrow SeCO + H_2$

$\Delta H = -0.07$ eV, $E_a = 1.96$ eV

Table 1 Reaction and associated energies in eV.

Reaction	Energy (eV)	Reaction	Energy (eV)
$SeCO + H_2Se \rightarrow SeCSeHOH$	0.66	$CO+H_2Se \rightarrow OCH_2Se$ (TS)	1.96
$SeCO + 3H_2 \rightarrow H_3CSeH + H_2O$	-1.27	OCH_2Se (TS) $\rightarrow SeCO + H_2$	-2.03
$CO + Se_2 \rightarrow SeCO + Se$	1.14	$SeCOH + HSe \rightarrow SeCO + H_2S$	-3.22
$CO + Se \rightarrow SeCO$	-3.62	$CH_4 + Se_2 + CSe_2 + 2H_2$	4.01
$SeCO + H_2Se + CSe_2 + H_2O$	0.54	$CO + H_2Se + SeCO + H_2$	-0.07
$SeCSeHOH \rightarrow CSe_2 + H_2O$	2.90	$SeCO + H_2Se \rightarrow SeCOH + HSe$	3.22
$CO + HSe \rightarrow SeCOH$	0.90	$CO + H_2Se \rightarrow OCH + HSe$	2.42
$H_3CSeH + H_2 \rightarrow CH4 + H_2Se$	-0.90	$CO+HSe \rightarrow SeCO + 1/2H_2$	1.18
$SeCOH + HSe \rightarrow SeCSeHOH$	-2.56	$CH_2 + H_2Se \rightarrow CH_3+HSe$	-1.58
$CH3_3 + HSe \rightarrow H_3CSeH$	-2.65	$CH_3+ H_2Se \rightarrow CH_4+HSe$	-1.30
$CH_4 + 2H_2Se \rightarrow CSe_2+ 4H_2$	6.34	$CH_4 + 2Se_2 \rightarrow CSe_2 + 2H_2Se$	3.24

II) Then, SeCO interacts with H_2 gases and converts to

$SeCO + 3H_2 \rightarrow H_3CSeH + H_2$

III) Then H_3CSeH degrades to CH_4 by releasing water and H_2 gases to the environment.

$H_3CSeH + H_2 \rightarrow CH_4 + H_2Se$

IV) At elevated temperatures, CSe_2 is expected to form in the presence of CH_4 and Se_2.

$CH_4 + 2Se_2 \rightarrow CSe_2 + 2H_2Se$

In the case of the methane interaction with Se radical, the two consecutive insertion reactions of Se in the H-C bond, followed by two H_2 releases (Eqs. 5-6) can also lead to the CSe_2 formation but this pathway is kinetically hindered because of a fairly high energy barrier:

$$CH_4 + Se \rightarrow HSe\text{-}CH_3 \rightarrow Se{=}CH_2 + H_2 \qquad (5)$$

$$Se{=}CH_2 + Se \rightarrow Se{=}CH(SeH) \rightarrow CSe_2 + H_2 \qquad (6)$$

Lastly, H_2 molecules released during the CO methanation can hydrogenate Se-atoms to form H_2Se.

$2H_2 + 2Se \rightarrow 2\ H_2Se$

As a result, all these DFT results together suggest the formation of the stable byproducts of CSe_2, H_2, H_2Se, HSe, H_2O, CH_4 during the MOCVD reactions

3.2. By-products derived from chemical reactions of the precursors $W(CO)_6$ and H_2Se using ReaxFF simulations

In this section CVHD method is combined with ReaxFF-MD simulations to shed a light on the elementary reaction pathways and the kinetics of the byproducts formed during the MOCVD growth from the gas precursors $W(CO)_6$ and H_2Se. Molecular dynamics (MD) simulations are highly effective in capturing detailed chemical events, reaction pathways, and product formation during gas-phase simulations. However, the MD timescale is usually restricted to nanoseconds, but the occurrence of meaningful reactions encountered during experiments usually require a timescale of about seconds to minutes [22]. Therefore, the traditional MD method employs high temperature to accelerate molecular collisions and successful reaction events. To address this discrepancy between the temperature used in MD simulations and experimental conditions, several accelerated molecular dynamics methods have been developed [23]. Collective Variable-driven Hyperdynamics or

CVHD [24, 25] is one of these methods which combines hyperdynamics and metadynamics to accelerate reactive events. Using this method, the MD simulation is performed by adding a bias potential $\Delta V(\eta)$ to the true potential energy surface to overcome the energy barrier in low-temperature simulations. The bias is constructed dynamically and is a function of collective variables (CVs) based on a distortion function described as $\chi_i = (r_i - r_i^{min})/(r_i^{max} - r_i^{min})$ where r_i is the length of every pair of bonds and $r_i^{min}$and r_i^{max} denotes the bond length of pair $i$at the beginning and end of a reaction event. The effective simulation time which is referred to as 'hypertime', is the multiplication of boost factor with the MD simulation time: $t_{hyper} = t_{MD} \times Boost = t_{MD} \times \langle e^{\beta\Delta V(\eta)} \rangle$ where $\beta = 1/k_B T$ and k_B is the Boltzmann constant.

The simulation box consisted of 1 $W(CO)_6$ and 20 H_2Se with the dimensions of 30x30x30 Å^3 (Figure 4a). The system energy was minimized and heated up to the target temperature of 1500 K with a heating rate of 50K/ps and an increment of 100 K with a time step of 0.1 fs. Each temperature increment was followed by an equilibration of 100ps. CVs are based on the distortion of local bond lengths and this study included three types of bonds for constructing CVs. The first one is W-Se bond with parameters $r_i^{min} = 2.10$Å and $r_i^{max} = 3.05$Å and the second pair is the H-Se bond with $r_i^{min} = 1.50$Åand $r_i^{max} = 2.80$Å and C−O bond with $r_i^{min} = 1.20$Åand $r_i^{max} = 2.50$Å. The $r_i^{min}$and r_i^{max} values are based on the potential energy versus bond scan data available in Ref.17. Gaussian hills of width δ=0.025 and height ω = 0.25 kcal/mol were deposited at an interval of 1000 iterations (t_i = 0.1ps) and the waiting time to check if a reaction occurred is 1ps as suggested in the reference.

As shown in Figure 4b, the chain reactions of the volatile $W(CO)_6$ and H_2Se precursors lead to the formation of the end product of WSe_3 at 1500 K. Additionally, based on the ReaxFF results, the stable by-products of CH_4, H_2Se, CO, H_2O, Se_2 and H_2 are expected to form during the MOCVD growth process (Figure 4b). It is noteworthy that the current ReaxFF potential does not completely capture the interaction between C and Se for the CSe_2 formation because this potential is not trained against the associated DFT data [17].

4. CONCLUSIONS

DFT and ReaxFF simulations have been conducted to explore details of the atomistic mechanism of $W(CO)_6$ and CO hydroselenization. The DFT results propose a thermodynamically favorable MOCVD reaction pathway which initiates from $W(CO)_6$ and H_2Se, and leads to the WSe_3 end product. Furthermore, both DFT and ReaxFF results show that the conversion of $W(SeH)_2Se_2$ to WSe_3 is entropy driven, meaning that such conversion needs elevated temperatures (e.g. heating system at elevated temperature) to eliminate H_2Se from the energetically more stable $W(SeH)_2Se_2$. H_2 release reactions are also expected to play a crucial role in the MOCVD growth of WSe_2. The results presented here indicate that H_2 elimination from $W(CO)_4(H_2Se)_2$ requires the highest activation energy, and as such is considered as a rate-limiting reaction governing the MOCVD growth kinetics. Both ReaxFF and DFT results suggest the formation of stable byproducts of CSe_2, H_2, H_2Se, HSe, H_2O, CH_4 besides the end product of WSe_3 during the MOCVD chemical reactions at elevated temperatures. Since understanding the MOCVD gas-phase kinetics is critical to fabricate large-area single crystal transition metal diselenide thin film, this work can provide valuable thermodynamic and kinetic insight into the $W(CO)_6$ and CO hydroselenization in chalcogen rich environment.

Acknowledgments

This work was financially supported by the National Science Foundation (NSF) through the Pennsylvania State University 2D Crystal Consortium−Materials Innovation Platform (2DCC-MIP) under the NSF cooperative agreement DMR-1539916. The author also thanks Prof. Adri van Duin for the fruitful discussions

REFERENCES

[1] A. Eftekhari, “Tungsten Dichalcogenides (WS_2, WSe_2, and WTe_2): Materials Chemistry and Applications,” J. Mater. Chem. A, vol. 5, no. 35, pp. 18299–18325, 2017

[2] T.H. Choudhury, X. Zhang, Z.Y.A. Balushi, M. Chubarov, J.M. Redwing, “Epitaxial Growth of 2D Layered Transition Metal Dichalcogenides,” ArXiv190903502 Cond-Mat 2019.

[3] H. Qin, Q.-X. Pei, Y. Liu, Y.-W. Zhang, “The Mechanical and Thermal Properties of MoS2–WSe2 Lateral Heterostructures,” Phys. Chem. Chem. Phys., vol. 21, no. 28, pp. 15845–15853, 2019.

[4] W. Choi, N. Choudhary, G.H. Han, J. Park, D. Akinwande, Y.H. Lee, “Recent Development of Two-Dimensional Transition Metal Dichalcogenides and Their Applications,” Mater. Today, vol. 20, no. 3, 116–130, 2017.

[5] D. Andrzejewski, H. Myja, M. Heuken, A. Grundmann, H. Kalisch, A. Vescan, T. Kümmell, G. Bacher, “Scalable Large-Area p–i–n Light-Emitting Diodes Based on WS2 Monolayers Grown via MOCVD,” ACS Photonics, vol. 6, no. 8, pp. 1832–1839, 2019.

[6] X. Zhang, F. Zhang, Y. Wang, D.S. Schulman, T. Zhang, A. Bansal, N. Alem, S. Das, V.H. Crespi, M. Terrones, J.M. Redwing, “Defect-Controlled Nucleation and Orientation of WSe_2 on HBN: A Route to Single-Crystal Epitaxial Monolayers,” ACS Nano, vol. 13, no. 3, pp. 3341–3352, 2019.

[7] B.D. Keller, A. Bertuch, J. Provine, G. Sundaram, N. Ferralis, J.C. Grossman, “Process Control of Atomic Layer Deposition Molybdenum Oxide Nucleation and Sulfidation to Large-Area MoS_2 Monolayers,” Chem. Mater., vol. 29, no. 5, pp. 2024–2032, 2017.

[8] W. Hao, C. Marichy, C. Journet, “Atomic Layer Deposition of Stable 2D Materials,” 2D Mater., vol. 6, no. 1, 012001, 2018.

[9] G.-H. Park, K. Nielsch, A. Thomas, “Atomic Layer Deposition: 2D Transition Metal Dichalcogenide Thin Films Obtained by Chemical Gas Phase Deposition Techniques (Adv. Mater. Interfaces 3/2019),” Adv. Mater. Interfaces, vol. 6, no. 3, 1970024, 2019.

[10] X. Zhang, Z.Y. Al Balushi, F. Zhang, T.H. Choudhury, S.M. Eichfeld, N. Alem, T.N. Jackson, J.A. Robinson, J.M. Redwing, “Influence of Carbon in Metalorganic Chemical Vapor Deposition of Few-Layer WSe_2 Thin Films,” J. Electron. Mater., vol. 45, no. 12, pp. 6273–6279, 2016.

[11] T.H. Choudhury, H. Simchi, R. Boichot, M. Chubarov, S.E. Mohney, J.M. Redwing, “Chalcogen Precursor Effect on Cold-Wall Gas-Source Chemical Vapor Deposition Growth of WS_2,” Cryst. Growth Des., vol. 18, no. 8, pp. 4357–4364, 2018.

[12] Y. Gong, X. Zhang, J.M. Redwing, T.N. Jackson, “Thin Film Transistors Using Wafer-Scale Low-Temperature MOCVD WSe_2,” J. Electron. Mater., vol. 45, no. 12, pp. 6280–6284, 2016.

[13] L. Jiao, H.J. Liu, J.L. Chen, Y. Yi, W.G. Chen, Y. Cai, J.N. Wang, X.Q. Dai, N. Wang, W.K. Ho, M.H. Xie, “Molecular-Beam Epitaxy of Monolayer MoSe2: Growth Characteristics and Domain Boundary Formation,” New J. Phys., vol. 17, no. 5, 053023, 2015.

[14] Y. Zhang, T.-R. Chang, B. Zhou, Y.-T. Cui, H. Yan, Z. Liu, F. Schmitt, J. Lee, R. Moore, Y. Chen, H. Lin, H.-T. Jeng, S.-K. Mo, Z. Hussain, A. Bansil, Z.-X. Shen, “Direct Observation of the Transition from Indirect to Direct Bandgap in Atomically Thin Epitaxial $MoSe_2$,” Nat. Nanotechnol., vol. 9, no. 2, pp. 111–115, 2014.

[15] H.J. Liu, L. Jiao, L. Xie, F. Yang, J.L. Chen, W.K. Ho, C.L. Gao, J.F. Jia, X.D. Cui, M.H. Xie, “Molecular-Beam Epitaxy of Monolayer and Bilayer WSe_2: A Scanning Tunneling Microscopy/Spectroscopy Study and Deduction of Exciton Binding Energy,” 2D Mater., vol. 2, no. 3, 034004, 2015.

[16] M. Nakano, Y. Wang, Y. Kashiwabara, H. Matsuoka, Y. Iwasa, “Layer-by-Layer Epitaxial Growth of Scalable WSe_2 on Sapphire by Molecular Beam Epitaxy,” Nano Lett., vol. 17, no. 9, pp. 5595–5599, 2017.

[17] Y. Xuan, A. Jain, S. Zafar, R. Lotfi, N. Nayir, Y. Wang, T.H. Choudhury, S. Wright, J. Feraca, L. Rosenbaum, JM Redwing, V. Crespi, A.C.T. van Duin, “Multi-Scale Modeling of Gas-Phase Reactions in Metal-Organic Chemical Vapor Deposition Growth of WSe_2,” J. Cryst. Growth, vol. 527, 125247, 2019.

[18] A.D. Bochevarov, E. Harder, T.F. Hughes, J.R. Greenwood, D.A. Braden, D.M. Philipp, D. Rinaldo, M.D. Halls, J. Zhang, R.A. Friesner, “Jaguar: A High-Performance Quantum Chemistry Software Program with Strengths in Life and Materials Sciences,” Int. J. Quantum Chem., vol. 113, no. 18, pp. 2110–2142, 2013.

[19] Amsterdam Modeling Suite Making Computational Chemistry Work For You https://www.scm.com/ (accessed 2020 -11 -10).

[20] K. Chenoweth, A.C.T. van Duin, W.A. Goddard, “ReaxFF Reactive Force Field for Molecular Dynamics Simulations of Hydrocarbon Oxidation,” J. Phys. Chem. A, vol. 112, no. 5, pp. 1040–1053, 2008.

[21] K. Momma, F. Izumi, “VESTA 3 for Three-Dimensional Visualization of Crystal, Volumetric and Morphology Data,” J. Appl. Crystallogr., vol. 44, no. 6, pp. 1272–1276, 2011.

[22] S.M. Eichfeld, L. Hossain, Y.-C. Lin, A.F. Piasecki, B. Kupp, A.G. Birdwell, R.A. Burke, N. Lu, X. Peng, J. Li, A. Azcatl, S. McDonnell, R.M. Wallace, M.J. Kim, T.S. Mayer, J.M. Redwing, J.A. Robinson, “Highly Scalable, Atomically Thin WSe2 Grown via Metal–Organic Chemical Vapor Deposition,” ACS Nano, vol. 9, no. 2, pp. 2080–2087, 2015.

[23] K.L. Joshi, S. Raman, A.C.T. van Duin, “Connectivity-Based Parallel Replica Dynamics for Chemically Reactive Systems: From Femtoseconds to Microseconds,” J. Phys. Chem. Lett., vol. 4, no. 21, pp. 3792–3797, 2013.

[24] K.M. Bal, E.C. Neyts, “Merging Metadynamics into Hyperdynamics: Accelerated Molecular Simulations Reaching Time Scales from Microseconds to Seconds,” J. Chem. Theory Comput., vol. 11, no. 10, pp. 4545–4554, 2015.

[25] K.M. Bal, E.C. Neyts, “Direct Observation of Realistic-Temperature Fuel Combustion Mechanisms in Atomistic Simulations,” Chem. Sci., vol. 7, no. 8, pp. 5280–5286, 2016.